

*Letter to the Editor***High resolution observations of molecular outflows in the HH 1–2 region****J.C. Correia¹, M. Griffin¹, and P. Saraceno²**¹ Physics Department, Queen Mary & Westfield College, Mile End Road, London E1 4NS, UK² CNR - Istituto di Fisica dello Spazio Interplanetario, CP 27, I-00044 Frascati, Italy

Received 11 March 1997 / Accepted 25 March 1997

Abstract. We report $^{12}\text{CO J}=3-2$ high resolution observations of compact molecular outflows around VLA 1 and VLA 3, two young stellar objects in the HH 1–2 region. We have confirmed the existence of a new outflow associated with VLA 1, the powering source of these well known Herbig-Haro objects. The VLA 1 outflow exhibits red- and blue-shifted peaks with a separation of only $30''$. The two lobes are clearly distinct from each other, suggesting that the outflow axis is close to the plane of the sky. The outflow is aligned with the HH 1–2 axis, but the lobes are inside the HH knots. Our calculations have shown that this outflow is one of the weakest, youngest and most compact ever seen. Its total mass is $1.1 \times 10^{-3} M_{\odot}$ and the dynamical timescale is $\simeq 1 \times 10^3$ years. We have also mapped the more extended outflow from VLA 3 confirming the existence of two young, distinct and very compact molecular outflows in this region.

Key words: Stars: formation – Stars: pre-main sequence – ISM: individual objects: HH 1–2 – ISM: jets and outflows

1. Introduction

The well known Herbig-Haro objects, HH 1 and HH 2, the first objects of their class to be discovered (Herbig 1951; Haro 1952), are situated in L1641, a dark molecular cloud located in the southern part of the Ori A complex. L1641 is at a distance of 470 pc and it is known as a region of low- and intermediate-mass star formation.

HH 1 and HH 2, separated by $3'$, are moving in opposite directions (Herbig & Jones 1981) constituting a bipolar optical outflow, emanating from the powering source VLA 1, which lies midway between them (Pravdo et al. 1985).

Chernin and Masson (1995) mapped the region around VLA 1 in $\text{CO J}=2-1$ with $30''$ resolution and found an out-

flow with a red-shifted lobe which peaks at $(-0.8', 0.5')$ from VLA 1. The redshifted outflow lobe has a major axis with a position angle similar to the angle of 148° for the HH 1–2 axis. They claim that this outflow is powered not by VLA 1 but by VLA 3, a radio continuum source $1.3'$ to the north center of HH 1–2 flow, close to a H_2O maser. They did not detect any outflow associated with VLA 1 but suggested that higher resolution observations with a beam less than $0.25'$ would be necessary in order to separate out a possible weak HH 1–2 outflow from the strong VLA 3 outflow. They have estimated that they have only detected one-fourth of the material in the outflow that is moving at velocities significantly greater than the line width of the ambient cloud. With this correction, they derived a total mass of $0.3 M_{\odot}$ for the VLA 3 outflow. Any molecular outflow associated with VLA 1 would have to be extremely weak, and they estimated an upper limit of $0.03 M_{\odot}$ for its mass.

Ogura (1995) has reported the discovery of a pair of giant (linear size $\simeq 1$ pc) bow shock structures located symmetrically about HH 1–2. This was interpreted as an evidence for recurrent outflow activity of the exciting source. Further evidence is provided by the discovery that HH 1–2 is moving into a medium which is itself flowing at a speed of $\simeq 200 \text{ km s}^{-1}$ (Noriega-Crespo et al. 1989), suggesting a previous outflow in this region.

Recently, Choi et al. (1997) have reported observations of several molecular transitions around the HH 1–2 region. Their $\text{CO J}=3-2$ observations have indicated the presence of a weak molecular outflow in the VLA 1 area. The existence of the strong redshifted outflow from VLA 3 and the low resolution of their map around VLA 1 did not allow them clearly to identify VLA 1 as the powering source of the weaker outflow. The need for a larger map of $\text{CO J}=3-2$ around VLA 1 was pointed out by the authors.

2. Observations

The $^{12}\text{CO J}=3-2$ ($\nu = 345.796$ GHz) observations presented in this work were carried out in March and October 1994 at

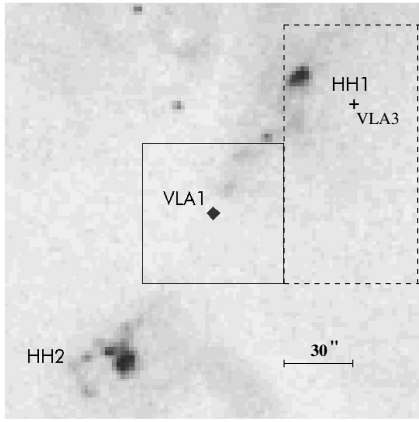


Fig. 1. The HH 1–2 region in the optical. The solid box represents the $1' \times 1'$ area centered in VLA 1 and mapped by us. This area is shown in Fig. 3. The dashed box corresponds to the area mapped by us around VLA 3. This area is shown in Fig. 5. The optical image was obtained using the Digitized Sky Survey from SkyView

the James Clerk Maxwell Telescope¹ (JCMT) on Mauna Kea, Hawaii. The $^{13}\text{CO } J=3-2$ ($\nu = 330.5881$ G Hz) observations were obtained during JCMT service time in November 1995. We used the B3i receiver in conjunction with the Dutch Autocorrelation Spectrometer (DAS). The beamwidth was $14''$ at 345 GHz. We integrated for several minutes per point, achieving typical rms noise levels of 0.1 K. The integration time for the $^{13}\text{CO } J=3-2$ observations was 30 minutes per point and typical rms noise levels of 0.02 K were obtained. These observations were done with the aim of estimating the optical depth of the ^{12}CO emission from the ratio of the ^{12}CO to the ^{13}CO intensities (see Goldsmith et al. 1984).

Figure 1 shows an optical image of the HH 1–2 region. The solid box represents the area around VLA 1 mapped by us in CO $J=3-2$ with $14''$ resolution. The $^{13}\text{CO } J=3-2$ data were obtained only on three positions around VLA 1. We have also mapped in CO $J=3-2$ an area of approximately $1' \times 2'$ around VLA 3. This area is shown as a dashed box in Fig. 1. Two positions were observed in $^{13}\text{CO } J=3-2$ in the direction of VLA 3.

3. Results

3.1. The VLA 1 outflow

Figure 2 shows the spectra at the central position and at two offset positions in the direction of VLA 1. The spectrum at the top corresponds to the peak of the red emission and the one in the middle shows the peak of the blue emission. The spectrum at the bottom is the one taken at the central position.

A map of the high-velocity $^{12}\text{CO } J=3-2$ emission in the direction of VLA 1 is shown in Fig. 3. The map is centered on VLA 1 (R.A. (1950) = $05^{\text{h}} 33^{\text{m}} 57^{\text{s}}$, DEC. (1950) = $-06^{\circ} 47'$

¹ The James Clerk Maxwell Telescope is operated by The Observatories on behalf of the Particle Physics and Astronomy Research Council of the United Kingdom, the Netherlands Organisation for Scientific Research and the National Research Council of Canada.

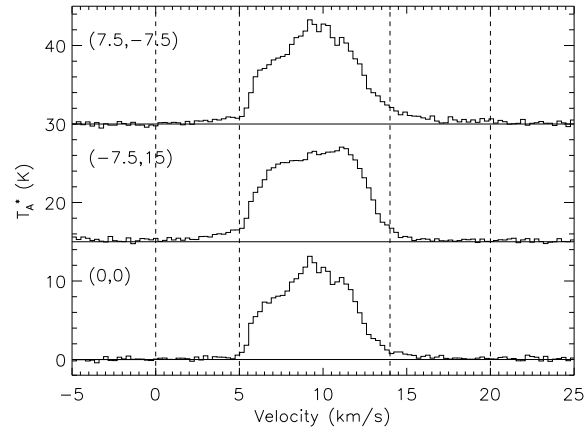


Fig. 2. Spectra of $^{12}\text{CO } J=3-2$ emission in the direction of VLA 1. The offset positions are shown at the top left corner in arcseconds relatively to VLA 1. For clarity, the top and the middle spectra are offset by 30 K and 15 K, respectively. The dashed lines show the velocity ranges over which we have integrated the high velocity emission

$55''$), covering an area of approximately $1' \times 1'$. A half beam spacing ($7.5''$) was used to cover the area and 49 positions were observed.

From the map we can see that the peaks of red- and blue-shifted emission are separated by only $30''$. However, the two lobes are clearly distinct from each other which suggests that the axis of the outflow is close to the plane of the sky. This axis is very well aligned with the HH 1–2 axis and VLA 1 is in the center of the two lobes. Taking into account our $14''$ beam size, we derive an angular diameter for the red lobe of $11''$ along the outflow direction and $10''$ along the direction perpendicular to it. The blue lobe has an angular diameter of $21''$ along the outflow direction but it is not resolved along the perpendicular direction.

We have also detected faint blue emission associated with the red lobe as well as faint red emission close to the blue lobe. This can be evidence for an interaction between the outflowing material and the ambient medium. An interaction between the outflow and the jet could lead to a re-direction of the outflowing material at the working surface of the jet (e.g. Padman et al. 1994), producing a component of emission in the opposite direction to the respective outflow lobe. Alternatively, this can be explained if we consider the outflow axis very close to the plane of the sky, as it seems to be the case. If the angle between the outflow axis and the plane of the sky is smaller than the outflow opening angle then we should expect to see, close to the blue lobe, some material receding from us; and for the same reason we should see some material approaching us when we look into the direction of the redshifted lobe.

Our $^{13}\text{CO } J=3-2$ observations were performed at the central position of VLA 1 and at the two offset positions corresponding to the peaks of the red and blue lobes in the $^{12}\text{CO } J=3-2$ map ($(7.5'', -7.5'')$ and $(-7.5'', 15'')$, respectively). We did not find any evidence for emission in the wings of the lines at a level of 0.02 K. The noise level achieved did not allow us to make

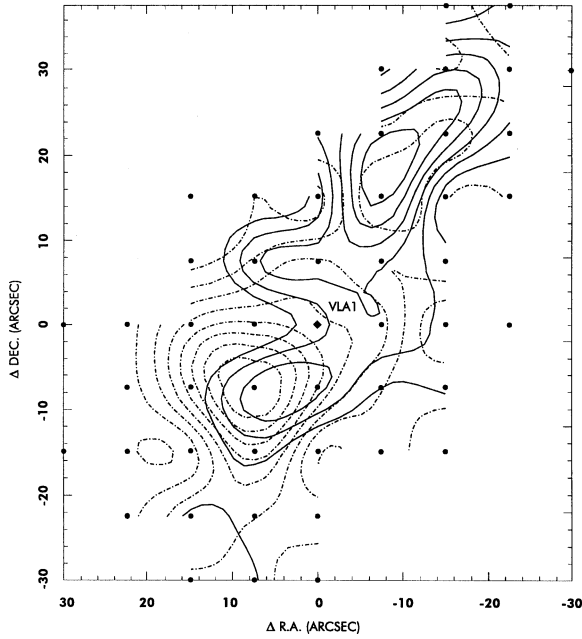


Fig. 3. CO $J=3-2$ map in the direction of VLA 1. Red-shifted emission is shown by dashed lines and corresponds to an integrated intensity between $14-20 \text{ km s}^{-1}$. Blue-shifted emission is shown by solid lines and corresponds to an integration between $0-5 \text{ km s}^{-1}$. The contour interval and the lowest contour are 0.5 K km s^{-1} . The dots show the 49 positions observed

an accurate estimative of the optical depth. However, 3σ upper limits were estimated and the results are: $\tau \leq 9$ and $\tau \leq 10$ for the red and blue lobes, respectively.

The mass, momentum and the energy of the CO $J=3-2$ outflow associated with each lobe have been calculated using the same approach taken by Scoville et al. (1986). We have adopted an excitation temperature (T_{EX}) of 30 K and we have considered optically thin emission. The results are summarized in Table 1. If the emission is optically thick, then these values increase by roughly a factor of τ . The dependence on the excitation temperature is weak (less than 1.6% for $20 < T_{EX} < 40 \text{ K}$). The momentum and energy values were calculated assuming that θ , the angle between the line of sight and the outflow axis, is 80° (Noriega-Crespo et al. 1991). The total mass associated with the outflow is $1.1 \times 10^{-3} M_\odot$ which is in accordance with the predictions made by Chernin and Masson (1995). This outflow is approximately 75 times less massive than the least massive outflow listed by Fukui et al. (1993). The existence of this outflow suggests that other sources that are currently classified as non-outflow sources might have very weak and compact outflows not yet detected (Saraceno et al. 1996).

From the outflow extent and the maximum velocity detected, we have estimated a dynamical timescale of $\simeq 1 \times 10^3 \text{ yr}$ for the outflow making this one of the youngest outflows ever detected.

3.2. The VLA 3 outflow

The spectrum obtained at the central position in the direction of VLA 3 is shown in Fig. 4 (bottom spectrum). This position was

Table 1. VLA 1 outflow physical parameters

	Mass (M_\odot)	Momentum ($M_\odot \text{ km s}^{-1}$)	Energy ($\times 10^{42} \text{ ergs}$)
Blue lobe	0.0003	-0.0092	3.44
Red lobe	0.0008	0.0366	16.5

Table 2. VLA 3 outflow physical parameters

	Mass (M_\odot)	Momentum ($M_\odot \text{ km s}^{-1}$)	Energy ($\times 10^{42} \text{ ergs}$)
Blue lobe	0.0192	-0.2337	34.1
Red lobe	0.0795	0.9692	143.0

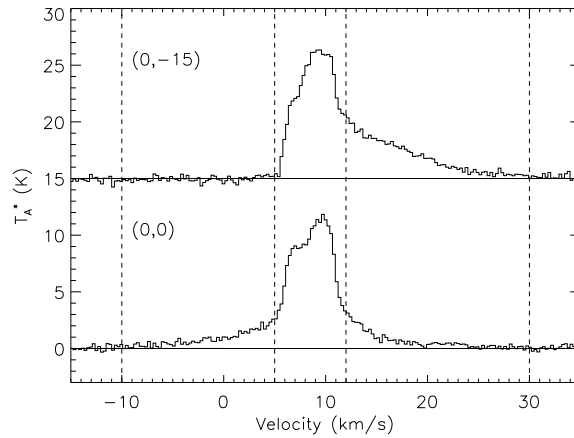


Fig. 4. Spectra of $^{12}\text{CO } J=3-2$ emission in the direction of VLA 3. The offset positions are shown at the top left corner in arcseconds. The upper spectrum is offset by 15 K for clarity. The dashed lines show the velocity ranges over which we have integrated the high velocity emission

identified as the position for which the blue emission achieves its peak. Fig. 4 also shows the spectrum for the offset position $(0'', -15'')$ where we clearly see very strong redshifted emission.

Figure 5 shows a map of the CO $J=3-2$ emission in the direction of VLA 3. It is clear that this outflow is much stronger and extended than the VLA 1 outflow. The blue peak is very close to VLA 3 and the two peaks are separated by only $20''$. The large overlap suggests that θ must be smaller than 45° .

We have taken $^{13}\text{CO } J=3-2$ spectra at the central position of VLA 3 and at the red peak position of the $^{12}\text{CO } J=3-2$ emission and, once again, we did not find any evidence of emission in the wings of the lines at a level of 0.02 K. The 3σ upper limits for the optical depth of the ^{12}CO emission are: $\tau \leq 1$ and $\tau \leq 6$ for the red and blue lobes, respectively. The strong restriction achieved for the red lobe is explained by the fact that very strong emission was detected in ^{12}CO (see Fig. 4) and no emission was detected in ^{13}CO ; this supports the hypothesis that the emission is also optically thin in the other lobes of both outflows.

The estimated physical parameters of the VLA 3 outflow are summarized in Table 2. We have again used $T_{EX} = 30 \text{ K}$ and we have considered optically thin emission. The momentum and

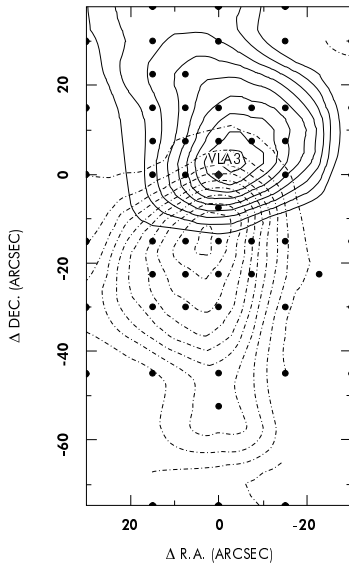


Fig. 5. Map of the CO J=3–2 emission in the direction of VLA 3. The red-shifted emission is shown as a dashed line and corresponds to an integrated intensity between 12 km s^{-1} and 30 km s^{-1} . The blue-shifted emission is shown as a solid line and corresponds to an integration between -10 km s^{-1} and 5 km s^{-1} . In the blue lobe, the lowest contour is 1 K km s^{-1} and the contour interval is 1 K km s^{-1} and in the red lobe the lowest contour is 2 K km s^{-1} and the contour interval is 2.5 K km s^{-1} . The dots show the 56 positions observed

energy values were calculated assuming $\theta = 45^\circ$. We estimate a dynamical timescale of $2.1 \times 10^3 \text{ yr}$.

4. Conclusions

We have presented $^{12}\text{CO J}=3-2$ high-resolution observations of the HH 1–2 region and our major conclusions are:

1. VLA 1 does indeed possess an outflow. This outflow is extremely weak, compact and young. We derived a total mass of $1.1 \times 10^{-3} M_\odot$ and a dynamical timescale of $\simeq 1 \times 10^3 \text{ yr}$. This outflow is clearly distinct from the stronger VLA 3 outflow. The existence of this outflow suggests that other sources that are currently classified as non-outflow sources might have very weak and compact outflows not yet detected.
2. VLA 3 is confirmed as a source with a more extended and powerful outflow. This outflow is almost 100 times more massive than the VLA 1 outflow.

Acknowledgements. Skyview was developed under NASA ADP Grant NAS5-31068 under the auspices of High Energy Astrophysics Science Archive Research Center (HEASARC) at the GSFC Laboratory for High Energy Astrophysics. The image on Fig. 1 is based on photographic data obtained using the UK Schmidt Telescope. The Digitized Sky Survey was produced at the Space Telescope Institute under US Government grant NAG W-2166. J. C. Correia is supported by a grant from JNICT – Programa PRAXIS XXI: BD/2961/94, Portugal.

References

- Chernin L., Masson C., 1995, ApJ 443, 181
 Choi M., Zhou, S., 1997, ApJ, (pre-print)
 Fukui Y., Iwata T., Mizuno A., et al., 1993. In: Levy E. H., Lunine J. I. (eds.) Protostars and Planets III. University of Arizona, Tucson, p. 602
 Goldsmith P. F., Snell R. L., Hemeon-Heyer M., et al., 1984, ApJ 286, 599
 Haro G., 1952, ApJ 115, 572
 Herbig G. H., 1951, ApJ 113, 697
 Herbig G. H., Jones B. F., 1981, AJ 86, 1232
 Noriega-Crespo A., Böhm K. H., Raga A. C., 1989, AJ 98, 1388
 Noriega-Crespo A., Calvet N., Böhm K. H., 1991, ApJ 379, 676
 Ogura K., 1995, ApJ 450, L23
 Padman R., Richer J. S., 1994, Ap&SS 216, 129
 Pravdo S. H., Rodriguez L. F., Curiel S., et al., 1985, ApJ 293, L35
 Saraceno P., André P., Ceccarelli C., et al., 1996, A&A 309, 827
 Scoville N. Z., Sargent A. I., Sanders D. B., et al., 1986, ApJ 303, 416